Laser trapping of deformable objects

Naoki Murazawa[1], Saulius Juodkazis[1], Hiroaki Misawa[1] and Hiroshi Wakatsuki[2]

[1]*Research Institute for Electronic Science, Hokkaido University, N21W10 CRIS Bldg., Sapporo 001-0021, Japan*

[2]*Asahi Glass Co., 1150 Hazawa-cho, Kanagawa-ku, Yokohama-shi, Kanagawa 221-8755, Japan*

saulius@es.hokudai.ac.jp; misawa@es.hokudai.ac.jp

Abstract: We report the trapping and manipulation of bubbles in viscous glass melts through the use of a laser. This phenomenon is observed in bubbles tens of micrometers in diameter under illumination by low numerical aperture ($NA = 0.55$). Once the bubble was centered on the optical axis, it was trapped and followed a lateral relocation of the laser beam. This phenomenon is explained by modifications of the bubble's shape induced by axial heating and a decrease in surface tension. It is shown that formation of a concave dimple on the bubble's front surface explains the observed laser trapping and manipulation. This mechanism of laser trapping is expected to take place in other deformable materials and can also be used to remove bubbles from melts or liquids. For this technique to be effective, the alteration of the bubble's shape should be faster than its expulsion out of the laser's point of focus.

OCIS codes: (070.4690) Optical morphological transformations; (140.7010) Trapping; (160.2750) Glass and other amorphous materials; (350.6980) Transforms

References and links

1. A. Ashkin, "Acceleration and trapping of particles by radiation pressure," Phys. Rev. Lett. **24**, 156–159, (1970).
2. D. G. Grier, "A revolution in optical manipulation," Nature **424**, 810–816, (2003).
3. D. McGloin, "Optical tweezers: 20 years on," Phil. Trans. R. Soc. A **364**, 3521–3537, (2006).
4. K. T. Gahagan and G. A. Swartzlander, Jr., "Optical vortex trapping of particles," Opt. Lett. **21**, 827–829, (1996).
5. P. A. Prentice, M. P. MacDonald, T. G. Frank, A. Cuschieri, G. C. Spalding, W. Sibbett, P. A. Campbell and K. Dholakia, "Manipulation and filtration of low index particles with holographic Laguerre-Gaussian optical trap arrays," Opt. Express **12**, 593–600, (2004).
6. J. Guck, R. Ananthakrishnan, H. Mahmood, T. J. Moon, C. C. Cunningham and J. Käs, "The optical stretcher: A novel laser tool to micromanipulate cells," Biophys. J. **81**, 767–784, (2001).
7. F. Wottawah, S. Schinkinger, B. Lincoln, R. Ananthakrishnan, M. Romeyke, J. Guck, and J. Käs, "Optical rheology of biological cells," Phys. Rev. Lett. **94**, 098103, (2005).
8. H. Misawa and S. Juodkazis, "Photophysics and photochemistry of a laser manipulated microparticle," Prog. Polym. Sci. **24**, 665–697, (1999).
9. S. Juodkazis, M. Shikata, T. Takahashi, S. Matsuo, and H. Misawa, "Fast optical switching by a laser-manipulated microdroplet of liquid crystal," Appl. Phys. Lett. **74**, 3627–3629, (1999).
10. S. Juodkazis, S. Matsuo, N. Murazawa, I. Hasegawa, and H. Misawa, "High-efficiency optical transfer of torque to a nematic liquid crystal droplet," Appl. Phys. Lett. **82**, 4657–4659, (2003).
11. Y. Nabetani, H. Yoshikawa, A. Grimsdale, K. Mullen, and H. Masuhara, "Laser deposition of polymer micro- and nanoassembly from solution using focused near-infrared laser beam," Jpn. J. Appl. Phys. **46**, 449–454, (2007).
12. M. P. MacDonald, G. C. Spalding, and K. Dholakia, "Microfluidic sorting in an optical lattice," Nature **426**, 421–424, (2003).
13. I. Smalyukh, D. Kaputa, A. Kachynski, A. Kuzmin, and P. Prasad, "Optical trapping of director structures and defects in liquid crystals using laser tweezers," Opt. Express **15**, 4359–4371, (2007).

#85299 - $15.00 USD Received 17 Jul 2007; revised 17 Sep 2007; accepted 23 Sep 2007; published 28 Sep 2007

14. S. Juodkazis, N. Mukai, R. Wakaki, A. Yamaguchi, S. Matsuo, and H. Misawa, "Reversible phase transitions in polymer gels induced by radiation forces," Nature **408**, 178–181, (2000).
15. A. Casner and J. P. Delville, "Giant deformations of a liquid-liquid interface induced by the optical radiation pressure," Phys. Rev. Lett. **87**, 054503, (2001).
16. S. Juodkazis, N. Murazawa, H. Wakatsuki, and H. Misawa, "Laser irradiation induced disintegration of a bubble in a glass melt," Appl. Phys. A **87**, 41–45, (2007).
17. M. Miwa, S. Juodkazis, and H. Misawa, "Drag of a laser trapped fine particle in a microregion," Jpn. J. Appl. Phys. **39**, 1930–1933, (2000).
18. A. Ashkin, "Forces of a single-beam gradient laser trap on a dielectric sphere in the ray optics regime," Biophys. J. **61**, 569–582, (1992).
19. J. Yamamoto, "On-demand optical tweezers using a liquid crystal spatial light modulator," Master Thesis of Hokkaido University, Japan. (2007).
20. J. A. Maroto, V. Pérez-Muñuzuri, and M. S. Romero-Cano "Introductory analysis of Bernard-Marangoni convection," Eur. J. Phys. **28**, 311-320, (2007).
21. K. Sasaki, M. Tsukima, and H. Masuhara, "Three-dimensional potential analysis of radiation pressure exerted on a single microparticle," Appl. Phys. Lett. **71**, 37–39, (1997).
22. S. Juodkazis, H. Misawa, O. Louchev, and K. Kitamura, "Femtosecond laser ablation of chalcogenide glass: explosive formation of nano-fibres against thermo-capillary growth of micro-spheres," Nanotechnology **17**, 4802–4805, (2006).

1. Introduction

Laser trapping and manipulation [1–3] has a growing number of applications in areas of science and technology in which particles and biomaterials from molecular to micrometer-size are to be individually imaged, manipulated, processed, modified, or deposited [4–12]. Tightly focused laser beams can be used to exert trapping (gradient) and pushing (scattering) forces on micro-objects and structures inside liquid crystals [13], gels [14], or liquid surfaces [15]. Though the laser trapping force is determined by the refractive indices of the environment and the object to be trapped, stable on-axis trapping occurs typically when using a tight focuse employing an objective lens with a numerical aperture of $NA > 1$. Also, the refractive index of the object should be larger than that of the surroundings, $n_o > n_s$. Hence, the laser trapping of a bubble in a glass melt ($n_o = 1, n_s = 1.57$) and at a $NA = 0.55$ focuse will not take place.

Here, we report on the experimental observation of laser trapping at low-NA and under a $n_o < n_s$ condition. This seemingly unusual phenomenon can be qualitatively explained by a change in the shape of a bubble, which responds to laser irradiation not as a rigid spherical particle but as a deformable object. For such trapping to occur, a change in the shape of the bubble should be faster than its expulsion from the point of focus.

2. Experimental

In this study, we used ABH61 and 1310Er Er-doped glasses (more details can be found in ref. [16]). There were no differences in regard to the laser manipulation of the bubbles in both types of glass. The glasses were heated and kept at 1000 $^\circ$C in a micro-oven (Japan HighTech Co., LTD; KL-1500) set on an up-right microscope (Nikon Optiphoto-2). Cw-laser radiation having a 1064 nm wavelength was used for trapping and manipulating the bubbles. The laser light was irradiated through an objective lens having a numerical aperture of $NA = 0.55$. The axial position of bubbles was determined by imaging and was set to be at least greater than the bubble's diameter from the sample's surface in order to avoid a dragging effect [17]. The viscosity of the melt at which the laser trapping of the bubbles was observed was 3.16 Poise. The glass melt had a free surface which was important for the convection initiated by laser heating. It was not possible to observe the side of the bubble in the current setup in which the sample placed inside the oven.

#85299 - $15.00 USD Received 17 Jul 2007; revised 17 Sep 2007; accepted 23 Sep 2007; published 28 Sep 2007

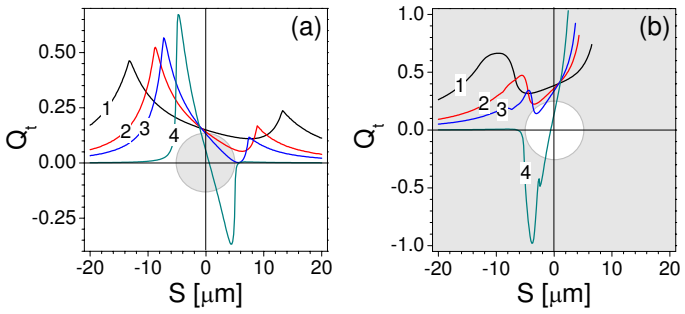

Fig. 1. The trapping force factor Q_t for a sphere $n_o = 2$ in water $n_o = 1.33$ (a), and for a bubble $n_o = 1$ in glass melt $n_o = 2$ (b). The laser trapping beam is focused along the Z axis at a position above $(+S)$ and below $(-S)$ the center of the sphere. The numerical apertures of the objective lenses are 0.5 (1), 0.75 (2), 0.9 (3), 1.3 (4); respectively, the input aperture is uniformly filled. Calculated by Eqs. (1), (2) [19]; $Q_t = Q_s + Q_g$, see text for details.

3. Theory: a rigid sphere

In our experiments, we trapped bubbles typically of a $10-20$ μm diameter. Hence, a theory based on geometrical optics is quantitatively applicable. The laser trapping force is a cumulative force composed of scattering (pushing) and gradient (trapping) elements, which are given by [18]:

$$F_s = \frac{n_s P}{c}\left[1 + R\cos 2\theta - \frac{\sin(2\theta - 2\varepsilon) + R\cos 2\theta}{1 + R^2 + 2R\cos 2\varepsilon}T^2\right] \tag{1}$$

$$F_g = \frac{n_s P}{c}\left[R\sin 2\theta - \frac{\sin(2\theta - 2\varepsilon) + R\sin 2\theta}{1 + R^2 + 2R\cos 2\varepsilon}T^2\right], \tag{2}$$

here P and c are power and the speed of light, θ and ε are the angles of incidence and the refraction of the light ray according to Snell's law $n_s \sin\theta = n_o \sin\varepsilon$, and R and T are the Fresnel reflection and transmission coefficients of the surface, respectively. Terms in brackets in Eqs. (1), (2) represent the scattering and gradient coefficients $Q_{s,g}$, respectively, with a cumulative coefficient being $Q_t = Q_s + Q_g$. The total force can be calculated by integrating the Eqs. (1), (2) over the angles filling the numerical aperture $NA = n\sin\theta$ [19]. The result is plotted as Q_t in Fig. 1.

Figure 1 shows the numerical results for the total force exerted onto a dielectric glass microsphere inside water (a common laser trapping condition) and for a bubble inside glass melt (as in our experiment). The $+S$ and $-S$ coordinates correspond to the position of a geometrical focus (without a micro-sphere) above and below the center. Stable trapping occurs when $F_g > F_s$, where the factor Q_t changes sign. There, a trapping potential, φ, defined by $F \equiv F_s + F_g = grad\varphi$, has its minimum. The restoring force around the central position can be well approximated by a Hookean law. A spherical particle having a high refractive index (Fig. 1(a)) can be trapped only at a high-NA ($NA > 1$) focuse since the high reflection makes the scattering larger than the gradient force. Objects with a lower refractive index contrast can be trapped even by a $NA < 1$ objective lens due to the small scattering force.

When a spherical particle with $n_o < n_s$ (Fig. 1(b)) is illuminated by a focused laser beam, the scattering force (positive) is dominant. This simulation is valid for a "rigid" bubble in a glass melt. The calculations shown in Fig. 1(b) were carried out until the total internal reflection (TIR) angle is obtained. Even at high-NA focusing, the bubble is attracted to the incoming beam (negative Q_t at negative S) when focused onto the bubble's front side. This is a direct

#85299 - $15.00 USD Received 17 Jul 2007; revised 17 Sep 2007; accepted 23 Sep 2007; published 28 Sep 2007

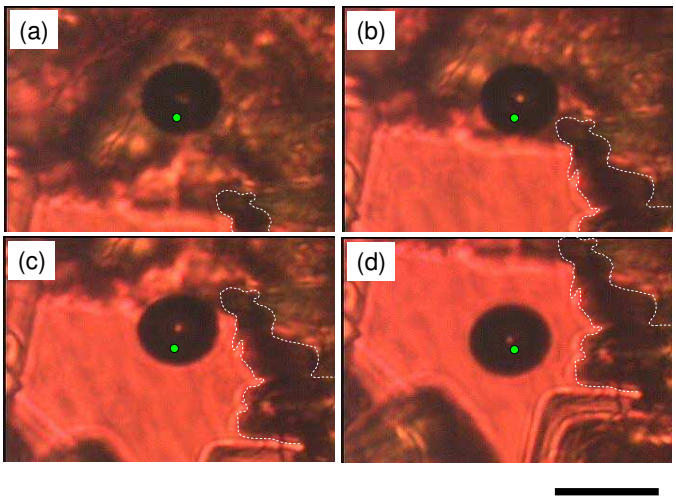

Fig. 2. Manipulation of a bubble inside a glass (ABH61) melt. Trapping laser power is 0.4 W; scale bar 20 μm. The dashed contour is a visual guide to recognize position change. The dot marks the focal position. The time difference between the frames is approximately 0.25 s.

consequence of the impulse change when the beam passes the boundary between two refractive index media [16]. The bubble is pushed out of focus axially at positive S. There is no stable trapping at $+S$ positions due to TIR. At lower NA, the bubble is also expected to be pushed out of focus ($Q_t > 0$). The calculations presented here are valid only for rigid micro-spheres and do not apply to our experimental conditions under which the bubbles were not "rigid" spheres as discussed below.

4. Results and Discussion

Figure 2 shows the manipulation of a bubble inside a glass melt. Moving a microscope stage after laser irradiation onto the bubble, it was fixated around the focus and appeared trapped and was laser manipulated. This contradicted the expected behavior of a low refractive index material inside a more optically dense medium as demonstrated in Fig. 1(b). Since the bubble was in constant movement, the focal spot was not centered on the bubble (Fig. 2). However, if the bubble was still, the laser focus could be centered on the object as expected (Fig. 3). The bubble shown in Fig. 3 entered the laser beam while it was driven by convection and the Brownian mechanism. The presence of convection is demonstrated by a movie clip (see, the supplement) in which the absorbing microparticles, most probably formed from phase-separated Bi in the melt of the same glass, are cyclically attracted and expelled out of the point of focus. The convection also affected bubbles and brought them towards the focus.

Experimental observations (Figs. 2-3) show that the bubble can be trapped and manipulated, in contrast to the expectations of a "rigid" sphere's behavior. We further explore the conjecture that the change in shape allowed for the laser trapping to occur.

The same arguments pertaining to ray tracing as used in the derivation of formulas Eqs. (1), (2) predict that the concave deformation on the spherical bubble would be required to facilitate trapping. It is noteworthy that such deformation is not optically recognizable from the axial direction shown in Fig. 2 and 3. The exact shape and size of the concave dimples are not considered here since no side-view images of the bubbles were available. However, a qualitative

#85299 - $15.00 USD Received 17 Jul 2007; revised 17 Sep 2007; accepted 23 Sep 2007; published 28 Sep 2007

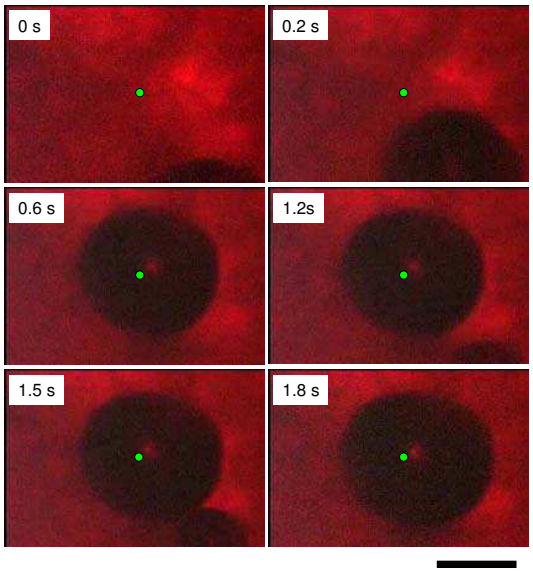

Fig. 3. Laser trapping of a bubble inside glass (1310Er) melt. After trapping a large bubble (frames at 0.6 - 1.5 s), coalescence with a smaller one occurred at 1.8 s. The laser trapping power was 0.4 W; scale bar 20 μm. The dot marks the focal position.

explanation of the trapping phenomenon can be inferred from this model as discussed below. Pinching of the bubble at the front and back side to form concave dimples has been predicted in ref. [16]. This pinching mechanism is due to the refractive index contrast between the object and its surroundings and has been shown to strech an object when the refractive index of the particle is larger than that of the surrounding medium [6].

Figure 4 shows 3D finite difference time domain (FDTD) simulations of a Gaussian laser beam propagated through the interior of the dumbbell- and spherical-shaped bubbles inside glass at different geometries. The dumbbell-shaped bubble was modeled as a sphere with on-axis concave dimples. The concave dimples were modeled as a sphere since one would expect the surface tension force to be dominant in their formation. The exact shape and size would affect only the total trapping force and the stiffness of the laser trap. The focuse was the same as that used in our experiments. The on-axis dumbbell-shaped bubble has a laterally stable location when laser tweezers are set on the bubble. If such a bubble would move sideways (a 1.2 μm vertical shift is modeled in Fig. 4), a restoring force would be generated to re-center the dumbbell-shaped bubble. This is evidenced by the change in direction of the intensity field: a downward-pointed intensity distribution pushes the bubble upwards and vice versa. If the same side-shift would occur for a spherical bubble it would be pushed out of focus, as is visualized in Fig. 4. It is noteworthy that only the front-side concave dimple is essential for laser trapping under the present focusing conditions since light intensity is much weaker on the back-side of the bubble. Hence, its shape has only a minor effect on trapping.

This axial trapping can be explained by the convex-to-concave transformation of the front surface. Such transformation is equivalent to the increase of the incidence angle or numerical aperture in the simulations shown in Fig. 1(b). At large NA, the bubble is expected to be pulled. For such surface deformation to take place the surface tension at the bubble rim should be low and the mass transfer between hot and cold regions should be efficient. For the mass transfer

#85299 - $15.00 USD Received 17 Jul 2007; revised 17 Sep 2007; accepted 23 Sep 2007; published 28 Sep 2007

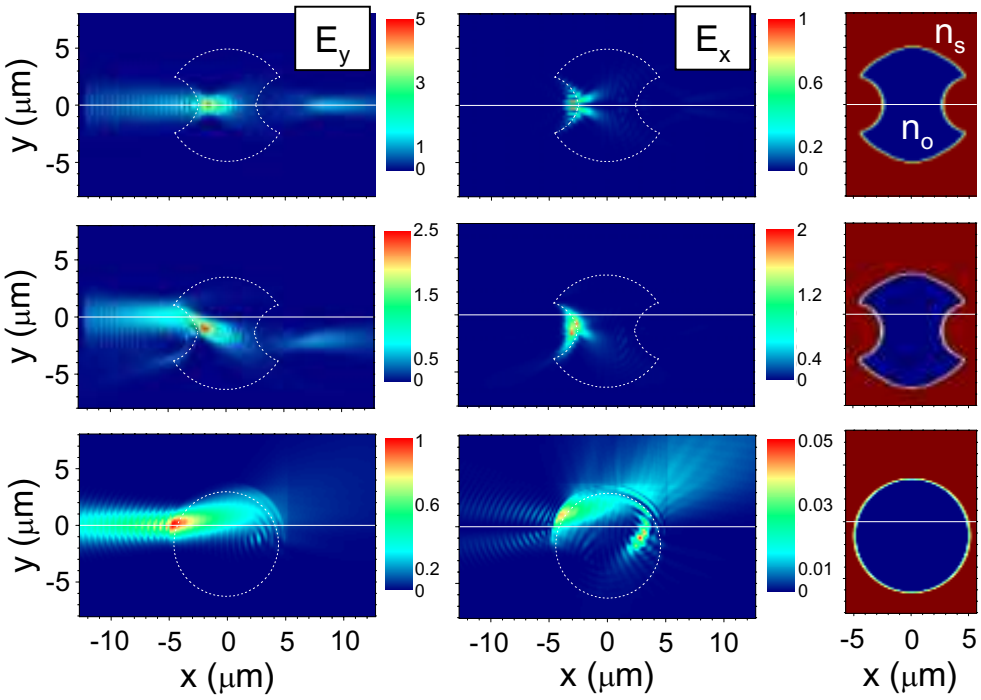

Fig. 4. Central cross sections of the intensity distributions of E_y^2 and E_x^2 components along with the refractive index (glass $n_s = 1.5$ and bubble $n_o = 1$) for different bubble and irradiation geometries (see text for details). The incident Gaussian beam (the field components are $(0,1,0)$) propagated along the x-axis and was focused at the $(0,0)$ position. The outline of shape-modified bubble is shown by a dashed line.

by the surface tension force to dominate a Marangoni number, $M = |\frac{d\sigma}{dT}|\Delta T d/(\rho \nu \kappa)$, should be larger than the critical value of 81 [20], here ρ is the mass density, ν the dynamic viscosity, κ the thermal diffusivity, d the thickness of the film (the diameter of the bubble in our case), $\frac{d\sigma}{dT}$ the temperature derivative of surface tension, and ΔT the temperature gradient over the thickness d. Conservative estimates predict $M \simeq 10^3$ for our experiments (here we consider $\Delta T < 100$ K which is much less than the temperature increase observed in smaller bubbles under the same irradiation conditions with ΔT = 850 K [16]). Hence, the surface modification under non-uniform heating together with a pinching force acting on the front and back sides of the bubble [16] and Marangoni flow, is consistent with the change in shape and the formation of a concave dimple on the bubble's front surface. A concave front surface is required for axial trapping and it is equivalent to a large NA irradiation as shown in Fig. 1(b) at the largest NA.

It is informative to explore the locations in which the changes in light intensity occur and their maximum values since changes in the surface tension of molten glass is key to the understanding of the mechanism of the observed trapping phenomena. The decrease of surface tension ($\sigma \propto T^{-1}$) facilitates deformation of the bubble and is expected to occur by the absorption of laser radiation at the locations in which the radiation shows high intensity. The maximum of intensity for the on-axis dumbbell-shaped irradiation is located just behind the glass/bubble's boundary inside the bubble. For the out-off-axis irradiation the maxima of the E_y^2 and E_x^2 components are inside glass at the bubble's rim. There is a considerable enhance-

#85299 - $15.00 USD Received 17 Jul 2007; revised 17 Sep 2007; accepted 23 Sep 2007; published 28 Sep 2007

ment of intensity components near the edge (moreover, there were no E_x components in the incident light). A local increase in temperature takes place in the presence of absorption in the glass and in heated vapor inside the bubble. We have recently determined that such a heating mechanism was responsible for a temperature of 1850 °C when the same molten glass was kept in a 1000 °C oven [16]. When the spherical bubble is illuminated by a focused laser beam (Fig. 4), the maximum intensity is also at the bubble/glass edge. Hence, in order for the bubble to be trapped, the transformation of the bubble's shape should be faster that the bubble's viscous response time, as discussed below.

The viscous response time of the spherical particle in solution is $\tau_R = (4\pi r^2 \rho/(9\eta))^{-1}$ [21], where r and ρ are the radius and mass density of the particle, respectively, and η is the dynamic viscosity of solution. The estimated τ_R value for our experimental conditions is ≈ 1 μs. Hence, the heating and surface tension-induced flow of molten glass should occur faster in order for the shape change to take place before the bubble is pushed out of the point of focus. The time scale of the molten glass's viscous flow can be estimated by $\tau_f \approx l^2/\nu$, where $l \sim 1$ μm is the characteristic size comparable with the waist of the beam and $\nu \approx 10^{-7} - 10^{-6}$ m^2/s is the kinematic viscosity of high temperature melts. Then, $\tau_f \approx 1 - 10$ μs [22] is of the same order as the viscous response time of the "rigid" bubble. Hence, it is conceivable that the bubble's shape is modified before the bubble is pushed out.

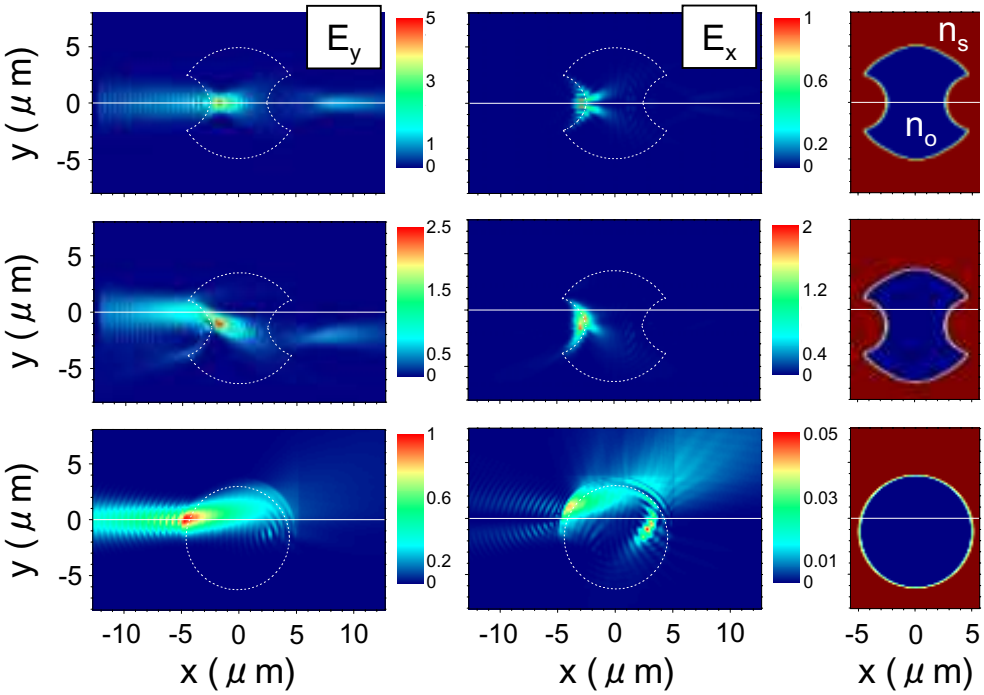

Fig. 5. Description of the movie clip file of the Supplement (file size : 3.6MB). Evidence of convection inside a ABH61 glass melt created by irradiation by a tightly focused ($NA = 0.55$) laser beam of 0.4 W power at a 1064 nm wavelength. The temperature of the oven in which the glass sample was kept was 1000°C. The absorbing microparticles, most probably formed from a phase-separated Bi in the melt, are cyclically attracted and expelled out of the point of focus. The horizontal side length of the video frame is 65 μm.

#85299 - $15.00 USD Received 17 Jul 2007; revised 17 Sep 2007; accepted 23 Sep 2007; published 28 Sep 2007

This mechanism of the trapping of bubbles by a laser at low-NA illumination can be observed only in a viscous medium and under low surface tension conditions, which facilitate the bubble's change in shape. This phenomenon is expected to take place in various materials close to phase transitions, e.g., in liquid crystals and gels.

5. Conclusions

We demonstrate that a bubble can be trapped in a glass melt at a low-NA focuse. The mechanism of this observation we explained by numerical modeling confirming that a bubble with a concave dimple can be fixed at the laser's focal point. A low surface tension is shown to be responsible for trapping and deforming the bubble's shape.

Acknowledgments

SJ acknowledges the partial financial support provided by a Grant-in-Aid from the Ministry of Education, Science, Sports, and Culture of Japan, No.19360322.

#85299 - $15.00 USD Received 17 Jul 2007; revised 17 Sep 2007; accepted 23 Sep 2007; published 28 Sep 2007